

Anthropogenic Climate Change: What the data shows

Anonymous

Department of Physics, University of Toronto, M5S 1A7 Toronto, Ontario, Canada

(Received 8 March 2025; peer reviewed XX Month 2025; submitted XX Month 2025)

The effect of carbon dioxide in the atmosphere as a greenhouse gas is well understood and has been well studied since the second half of the XIXth century^{1,2}. Since the Industrial Revolution, each step of the global carbon cycle has been disrupted - from fossil fuels to deforestation and industrial emissions - causing surface and air temperature increases large enough to impact the Earth's climate. The greatest indicators of climate change are rising sea levels, melting ice caps, and increase in surface temperatures. By analysing their data, provided by institutions and researchers, the impact of climate change is quantified. Further discussion on national carbon emissions over the last century is included to examine global trends in carbon emissions.

I. Introduction

Pre-industrial carbon emissions into the atmosphere are attributed to the global carbon cycle. Natural sources of CO₂ were limited to natural fires, wildlife activity, and decaying carbon life. Natural sources of carbon sinks were the fossilization of organic matter, permafrost, soils, surface sediments, organic matter, and dissolved inorganic carbon in bodies of water, with the remaining carbon being in the atmosphere. The emission of carbon caused by industrial processes and land-use change from anthropogenic activity cause an imbalance in the carbon cycle which cannot be balanced by natural processes such as dissolution into the oceans or absorption by organic matter, which grows or fossilizes³. As per Friedlingstein et al.⁴, the imbalance in carbon fluxes from 2011-2020 averages per year is of -0.3 GtC.

The atmosphere is mainly composed of nitrogen (77%) and oxygen (20.5%), with water vapour making up 2.5% and carbon dioxide only 0.04%. The increase in CO₂ levels caused by anthropogenic activity varies on geological factors, such as local fauna and flora densities, as well as human activity. As such, measurements of atmospheric CO₂ concentrations will differ geographically. Different CO₂ densities will circulate through the atmosphere due to its circulation over the planet. Shown in Figure 1, the movement of the air varies depending on its latitude.

The impact of increasing CO₂ levels in the atmosphere on surface temperature can be quantified through the "climate sensitivity" which is the temperature change caused by a doubling of CO₂ levels in the atmosphere, Equation (1):

$$(1) \quad \Delta\theta = \theta(2\rho_{CO_2}) - \theta(\rho_{CO_2})$$

Where θ is the temperature and ρ_{CO_2} is the atmospheric concentration of CO₂.

The sea-level change can be attributed to an increase in volume of the ocean due to an increase in temperature, given by Equation (2)⁵:

$$(2) \quad \alpha = \frac{-1}{\rho} \frac{\partial \rho}{\partial \theta}$$

Where α is an experimental constant, ρ is the ocean's density, and θ is the ocean's temperature.

The volume of water in the oceans can be estimated using a sphere-model, where the oceans occupy 71% of the first 3700 km of the Earth's sphere, given by Equation (3):

$$(3) \quad V_{ocean} = \frac{4\pi(r)^3}{3} - \frac{4\pi(r-3700)^3}{3}$$

The atmospheric CO₂ concentration is measured by Equation (4):

$$(4) \quad \rho_{CO_2} = \frac{M_{CO_2, atm}}{M_{atm}}$$

Where M_{atm} is the mass of the atmosphere, estimated below:

$$(5) \quad F = M_{atm} \cdot g$$

$$(6) \quad P = \frac{F}{A} \Rightarrow M_{atm} = \frac{F}{g} = \frac{PA}{g} \quad (7)$$

Where $P = 101325 \pm 15000 \text{ Pa}$ at sea level and

$$g = 9.8066 \pm 0.030 \text{ N} \cdot kg^{-1}$$

The area of the Earth is given by Equation (8):

$$(8) \quad A = 4\pi r^2 = 510 \cdot 10^{14} \text{ m}^2$$

with $r = 6371.001 \pm (7.136/14.299) [\text{NSG}^1]$

Thus Eq. (7) calculates

$$M_{atm} = \frac{101325 \cdot 510 \cdot 10^{14}}{9.8066} = 5.24 \cdot 10^{18} \text{ kg}$$

$$\Delta M = M_{atm} \sqrt{\left(\frac{\Delta P}{P}\right)^2 + \left(\frac{2r\Delta r}{r^2}\right)^2 + \left(\frac{\Delta g}{g}\right)^2} = 7.769 \cdot 10^{17} \text{ kg}$$

$$\text{So } M_{atm} = (5.24 \pm 0.78) \cdot 10^{18} \text{ kg.}$$

The latitudinal gradient of emissions between measurements at the Mauna Loa Observatory and the South Pole Observatory is measured by Equation (9):

$$\Delta \rho_{CO_2} = \rho_{CO_2}(MLO) - \rho_{CO_2}(SPO).$$

The gross and net annual additions of carbon into the atmosphere from anthropogenic activities and natural sources is measured as:

$$(10) \quad C_{atm, gross} = (\text{fossil emissions excluding carbonation}) + \text{land-use change emissions.}$$

$$(11) \quad C_{atm, net} = C_{atm, gross} - (\text{ocean sink}) - (\text{land sink}) - (\text{cement carbonation}).$$

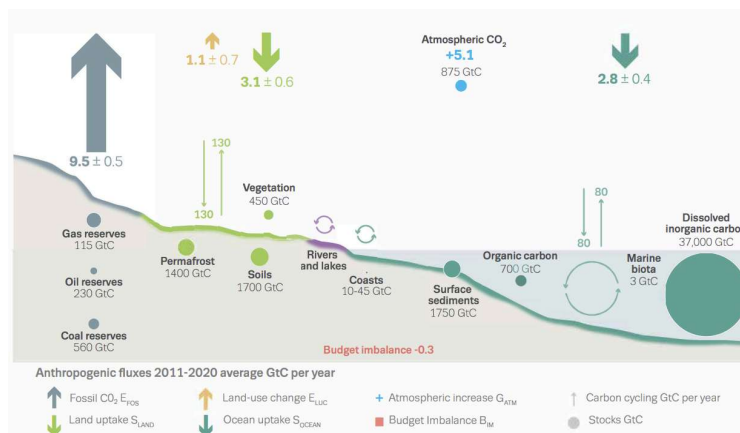


Figure 1: Schematic of the global carbon cycle. From Friedlingstein et al. Caption and figure from ACC-2023 Experiment Write-Up²⁰.

II. Methods

Measurements of the concentration of CO₂ in the atmosphere are performed by the National Oceanic and Atmospheric Administration (NOAA) Global Monitoring Laboratory (GML), on the Mauna Loa Volcano in Hawaii and at the South Pole Observatory in Antarctica. Data is obtained from NOAA's website^{7,8}, and was downloaded on March 17 2025 at 10:00am. Measurements for the global carbon cycle are provided by Friedlingstein et al. 2024⁴. The data provided by Friedlingstein et al. 2024 is a cumulation of other sources, which are described as such:

Emissions from fossil fuel combustion and industrial processes are provided by themselves, emissions from land-use change are averaged from four bookkeeping models. The atmospheric CO₂ growth rate is provided by NOAA's GML^{7,8}. The ocean sink is estimated from the average of 10 global ocean biogeochemistry models and the average of 8 ocean fCO₂ data products. The land sink is estimated from the average of 20 dynamic global vegetation models. The cement carbonation sink is averaged from two estimates.

III. Results

The gross and net annual additions of carbon into the atmosphere, $C_{atm, gross}$ and $C_{atm, net}$, are plotted in Figure 2

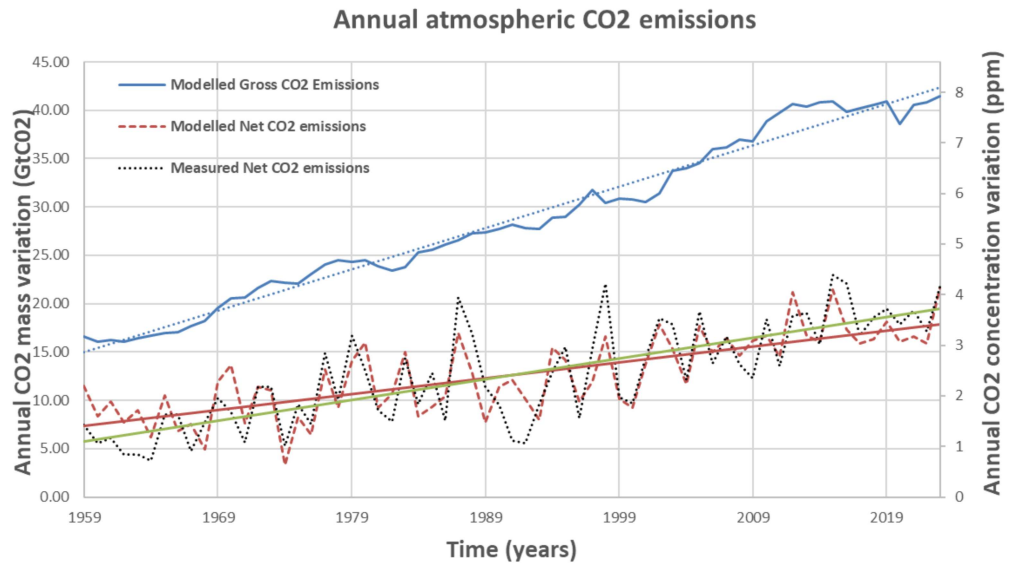


Figure 2: Annual variation in emitted CO₂ (gross and net) due to the global carbon cycle. Emissions are due to fossil fuel combustion and industrial processes as well as land-use change. Net emissions are lower due to the ocean and land sinks as well as cement carbonation. Linear fits are superimposed. All modelled data is obtained from Friedlingstein et al. 2024⁴, which also obtains the measured data from NOAA GML⁷.

Applying a linear model to the net emissions of CO₂ in Figure 2, the fit outputs:

$$(12) y \text{ (in GtC)} = 0.1643 x \text{ (in years)} - 314.57$$

The proven reserves of crude oil is of $1569.52 \cdot 10^9$ barrels as per OPEC Annual Statistical Bulletin 2024¹⁵. This converts to 674.89 GtCO₂ using EPA's 0.43 tCO₂/barrel conversion rate¹⁶. There are $1153.820 \cdot 10^9$ barrels of oil equivalent (boe) of gas reserves as of 2017 per BP's Statistical Review of World Energy¹⁷, and $5458.633 \cdot 10^9$ boe of coal as of 2016. This amounts to 496.14 GtCO₂ and 2347.21 GtCO₂ respectively. The fossil fuel emissions excluding carbonation trend to

$$(13) y \text{ (in GtC)} = 0.1236 x \text{ (in years)} - 239.7 \text{ where } y \text{ is annual CO}_2 \text{ mass variation in GtC rather than GtCO}_2.$$

Total emissions will be caused by burning all remaining fossil fuel reserves until they are depleted, at some time t_f :

$$\int_{2024+t_f}^{2024+88.80} (0.1236x - 239.7) = M_{reserves} = (674.89 + 496.14 + 3247.21)/3.6$$

The global sea level change is obtained from the United States Environmental Protection Agency (EPA)⁹, which uses data gathered by NOAA¹⁰ and the Commonwealth Scientific and Industrial Research Organisation (CSIRO)¹¹. The data is based on satellite and tide gauges measurements.

The surface temperature data is provided by the National Aeronautics and Space Administration Goddard Institute for Space Studies (GISS) Surface Temperature Analysis (GISTEMP v4)¹².

Data was sorted, filtered, and plotted using Python and the necessary libraries: SciPy, NumPy, and Matplotlib. All curve-fitting was done using NumPy's polyfit¹³, which performs a least squares polynomial fit, or using SciPy's curve-fit, which performs a non-linear least squares method to fit the data¹⁴. Missing or invalid data was replaced by the last valid value.

Where the conversion coefficient from GtCO₂ to GtC is $M_{co2} = 3.664 \cdot M_c$
This is solved for $t_f = 88.80$ years.

Therefore, the expected change in atmospheric CO₂ caused by using all the remaining fossil fuel reserves is calculated by using the linear emission model from past atmospheric emissions and projecting to $t_f = 88.80$ years:

$$(14) \Delta M_{co2} = \int_{2024}^{2024+88.80} (0.1236x - 239.7) = 2243.80 \text{ GtCO}_2.$$

Eq. (14) provides the total expected change in atmospheric CO₂ caused by using all the remaining fossil fuel reserves.

Mauna Loa⁷ and South Pole⁸ Observatories

Using NOAA's Mauna Loa daily measurements of atmospheric CO₂ mole fraction in ppm, the mean annual change in CO₂ is $1.908 \pm 0.123 \text{ ppm/year}$. For the South Pole data the annual change in CO₂ is $1.860 \pm 0.082 \text{ ppm/year}$. This was calculated as the mean of the yearly (jan-dec) averages. Data from Mauna Loa is shown in Figure 3.

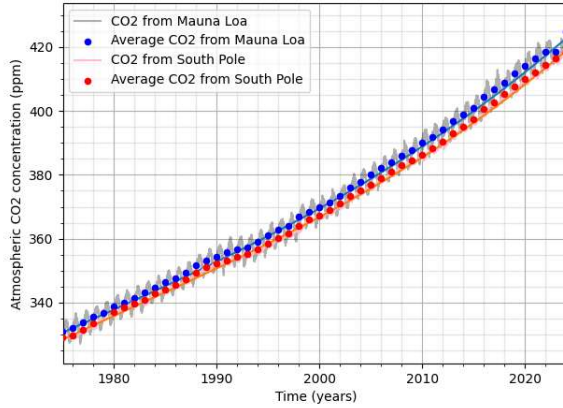


Figure 3: Mauna Loa and South Pole data. Data is fit to a 3rd degree polynomial fit and the shift is found using a least residuals where the residual is the difference between one fit shifted onto the other. Data from NOAA^{7,8}.

By checking which time shift in the Mauna Loa data best matches the South Pole data (both fit to 3rd degree polynomials), the shift of 1.49 years has the least residuals to the South Pole data. As such, the transport time is indicated to be 1.51 years for the CO₂ levels to catch up to Mauna Loa levels at the South Pole.

Since the South Pole has much lower presence of vegetation, the seasonal variation in CO₂ intake and uptake by vegetation and land-use change is not strong on seasonal time-period.

On the other hand, the Mauna Loa observatory is sampling air just 19.5°C North of the Equator, thus sampling air from the Central and Northern America, Europe and North Africa, Middle-East, and Asia, due to the movement of the air through Hadley and Ferrel Cells and the subtropical jet stream at 30°N North, shown below in Figure 4. As such, the seasonal variation from those relatively more vegetation affected regions in terms of atmospheric latitude and circulation is much more sensitive to seasonal vegetation changes which act as source and sinks of atmospheric CO₂.

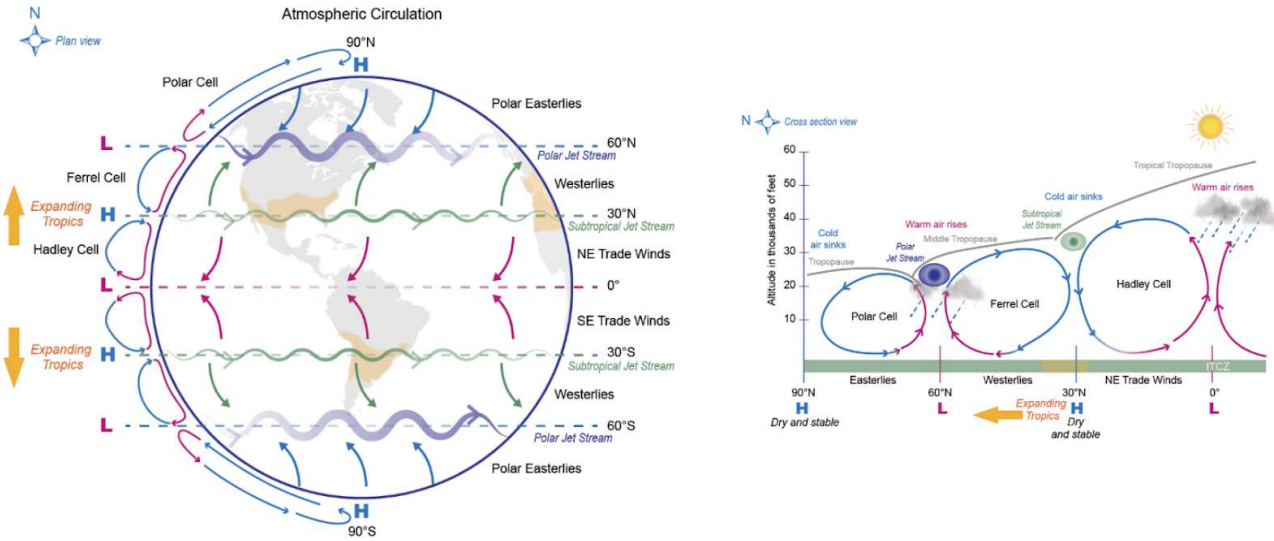


Figure 4: Conceptual view of the circulation in the atmosphere (top) on a sphere and (bottom) as a cross-section showing one hemisphere. Surface warming, predominantly over the equator, warms the air above and adds water from evaporation. The rising air leads to (L) low-pressure areas and cloud formation. Descending dry air leads to (H) high-pressure areas and desert formation. The circulation pattern repeats in the mid-latitudes in the Ferrel cell leading to complex weather systems at around 60 degrees latitude. Caption and figure from ACC-2023 Experiment Write-Up²⁰.

Generally, CO₂ levels tend to increase consistently, as human activity has remained productive since WW2 and most activity involves CO₂ emissions. Therefore, the largest events which may impact CO₂ levels only have minimal impacts.

After the necessary data adjustment to make them plottable (same-time scale and number of points), comparing the CO₂ emissions' latitudinal gradient versus the anthropogenic emissions shows clear correlation, given by the Pearson product-moment correlation coefficient of 0.8856 as calculated by NumPy's `correcoef()` tool. The quadratic and cubic fit do not provide much better χ^2 values (6.03, 5.92, 5.63 for the 1st, 2nd, and 3rd degree fits respectively) so the linear relation makes the most reasonable relation between the anthropogenic emissions and the latitudinal gradient of atmospheric CO₂. The two equations are:

$$(15) \Delta \text{CO}_2(\text{ppm}) = 0.110(\text{emissions (GtCO}_2)) - 0.78$$

$$(16) \Delta \text{CO}_2 = \text{CO}_2(\text{MLO}) - \text{CO}_2(\text{SPO})$$

Neglecting the adjustment factor of -0.78 ppm , the conversion factor for GtCO₂ to ppm units is of 0.110 ppm/GtCO_2 or $9.09 \text{ GtCO}_2/\text{ppm}$. From Figure 1, the average anthropogenic emissions per year are of $9.5 \pm 0.5 \text{ GtC}$ or $34.8 \pm 1.8 \text{ GtCO}_2$.

The average yearly atmospheric increase is of 5.1 GtC or 18.686 GtCO_2 which converts to $\frac{18.686 \text{ GtCO}_2}{5.24 \cdot 10^{10} \text{ Gt}} = 3.57 \text{ ppm}$ of added CO₂ every year from 2011-2020 averages.

This value is rather high when compared to the average yearly atmospheric increase given by Mauna Loa as 1.86 ppm/year . Considering Figure 4 indicates a total atmospheric CO₂ mass of 875 GtC or 611 ppm which is around 50% of what Mauna Loa measures, there must be some inconsistency in what is measured.

Surface Temperature

Using surface temperature data from the Goddard Institute for Space Studies (GISS) Surface Temperature Analysis version 4⁷, the global mean surface temperature has risen by 1.55 °C if we compare the yearly average of 1880 and 2023 respectively. Using a quadratic fit, shown in the plot of Figure 5, this difference between the endpoints (1880 to 2023) is of 1.15 °C.

From Figure 5, there is clear correlation between surface temperature changes and atmospheric CO2 abundance. By fitting both sets of data to a quadratic, the relationship between the two becomes clearly logarithmic in base 2, with a better χ^2 value for the logarithmic fit versus the linear fit. This is shown in Figure 6

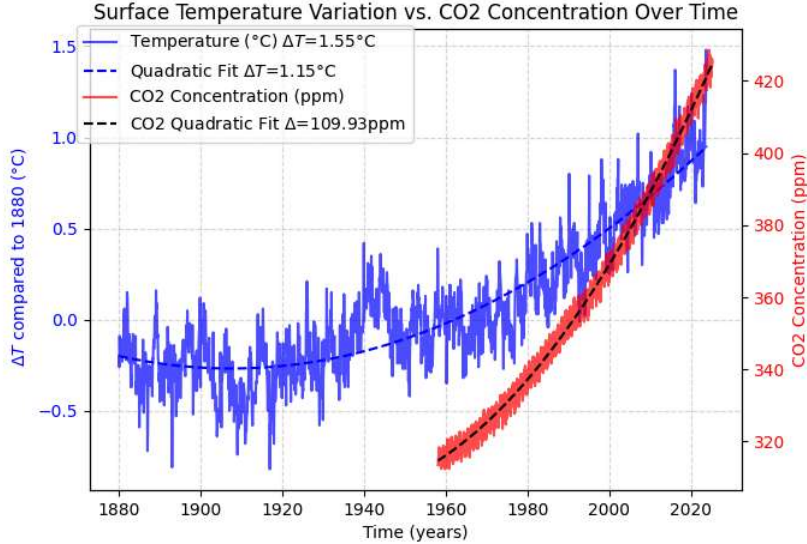


Figure 5: Global surface temperature variation with respect to 1880 plotted against time. On a secondary axis, the CO2 measurements of Figure 2 are plotted. Both functions are fit to quadratics. Data from GISTEMP¹² and NOAA⁷.

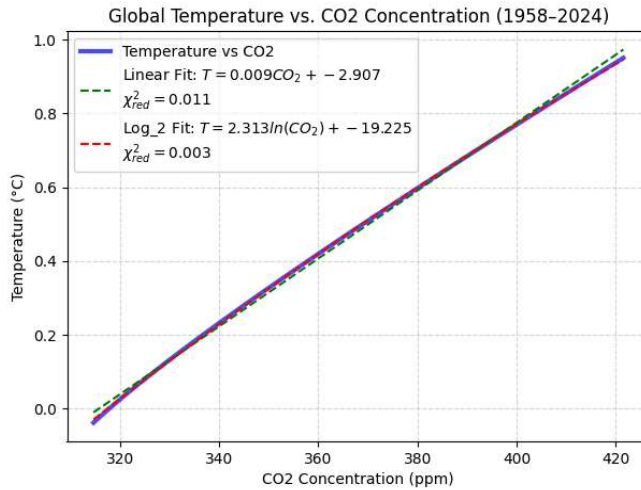


Figure 6: Mean surface temperature fit plotted against the atmospheric CO2 concentration fit. The best fit of the two quadratic fits (both plotted on Figure 5) against each other is a \log_2 function. Data from GISTEMP¹² and NOAA⁷.

Sea Level

The data from the EPA⁹ indicates a sea level change of +0.26m since 1880, which is in line with estimates from NASA and NOAA. A quadratic fit of the data suggests a total difference of 0.24 when comparing endpoints of the fit, with $\chi^2_{red} = 0.006$ considering uniform error ie $\sigma = 1$.

The climate sensitivity is estimated using the fit $T = 2.313\log_2(CO2)$ and Eq. (1):
 $\Delta T = T(2CO2) - T(CO2) = 2.313\log_2(2CO2) - 2.313\log_2(CO2)$
 $= 2.313(\log_2 2 + \log CO2) - 2.313\log_2(CO2) = 2.313^\circ C$
 IPCC reports estimate the climate sensitivity between 2-5°C, with the Sixth Assessment Report estimating 3°C.

$$(17) \quad \Delta V = \left(\frac{4\pi(r+\Delta r)^3}{3} - \frac{4\pi r^3}{3} \right) \cdot 0.71 = 9.42 \cdot 10^{12} m^3 \quad \text{where} \\ r = 6371 km \text{ and } \Delta r = 0.24m.$$

Thus we estimate that $\frac{\Delta V}{V_{GIS}} = \frac{9.42 \cdot 10^{12}}{\left(\frac{4\pi(r+\gamma)^3}{3} - \frac{4\pi r^3}{3}\right) \cdot 0.71} = 0.037 = 3.7\%$ of the

Greenland ice sheet volume would have to melt to be responsible for the 0.26m rise in sea levels, with an estimated sea level rise caused by melting the entire Greenland ice sheet of about 7m²⁰.

Additionally, the increase in ocean volume of $9.42 \cdot 10^{12} m^3$ from the 0.24m rise corresponds to:

$$V_{ice} = \Delta V \frac{\rho_{ocean}}{\rho_{ice}} = 9.42 \cdot 10^{12} \cdot \frac{0.99907}{0.9167} = 1.089\Delta V = 1.03 \cdot 10^{14} m^3$$

of ice, given their different densities¹⁸.

Using Eq. (2), we can find what increase in θ causes a rise Δr in sea levels for a given α , the thermal expansion coefficient (TEC). From Roquet et al., α varies from 0°C to 3°C depending on temperature, depth, and salinity. By examining their graphs of the TEC(α), values of α range from 0°C at the poles and 3.5 °C at the equator. Looking at climate model sensitivity to different α 's, it seems that $\alpha = 10^{-4} K^{-1}$ is a good value where models are not far off. As such:

$$\int_{\theta_i}^{\theta_f} \alpha d\theta = \int_{\rho_i}^{\rho_f} \frac{-1}{\rho} d\rho \Leftrightarrow \alpha \Delta \theta = -\ln(\rho_f) - (-\ln(\rho_i)) = \ln \frac{\rho_i}{\rho_f} = \ln \frac{V_f}{V_i}$$

where conservation of mass $V_i \rho_i = V_f \rho_f$ was used.

$$\Delta \theta = \frac{1}{\alpha} \ln \frac{\left(\frac{4\pi(r+0.259)^3}{3} - \frac{4\pi(r-3700)^3}{3}\right) \cdot 0.71}{\left(\frac{4\pi(r)^3}{3} - \frac{4\pi(r-3700)^3}{3}\right) \cdot 0.71} = \frac{1}{\alpha} \ln \frac{(r+0.259)^3 - (r-3700)^3}{(r)^3 - (r-3700)^3} = 0.70^\circ C.$$

Thus the ocean would have to heat up by 0.70°C to cause sea level rising of 0.26m. This assume $\alpha = 1 \cdot 10^{-4} K^{-1}$ and the ocean depth of 3700km can accurately depict a change in spherical volume of the ocean.

Who emits the most?

Using the data from Friedlingstein et al.⁴, the countries with the highest total cumulative emissions are:

1. USA: 82779 MtC
2. China: 63314 MtC
3. Russia: 28831 MtC
4. Japan: 16456 MtC
5. Germany 15816 MtC
6. India: 14136 MtC

When summing from yearly emissions from 1859 to 2020.

The results are much different for cumulative emissions per capita:

1. Estonia: 255 MtC/capita
2. Luxembourg: 290 MtC/capita
3. Trinidad and Tobago: 270 MtC/capita
4. USA: 250 MtC/capita
5. Czech Republic: 218 MtC/capita
6. Qatar: 204 MtC/capita
7. Brunei: 198 MtC/capita
8. Canada: 198 MtC/capita
9. Russia: 198 MtC/capita

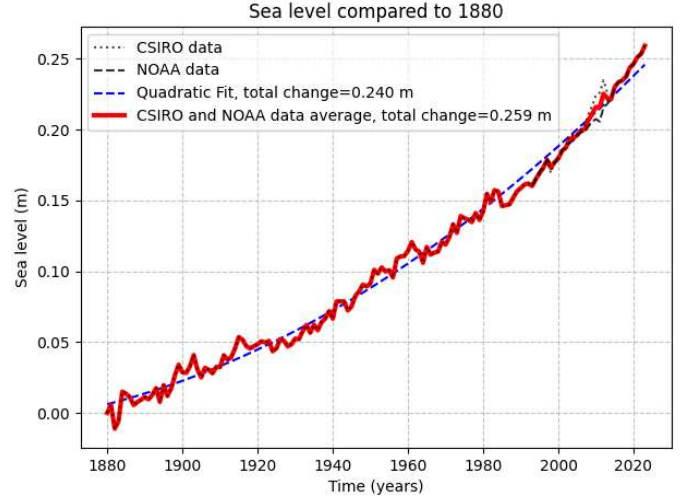


Figure 7: Sea levels compared to 1880, worldwide mean. Data from CSIRO¹¹ and NOAA¹⁰. Overlapping data was averaged, and otherwise simply combined, before being fit to a quadratic function

Where the population data was obtained from the World Bank¹⁹. A mix of strong economies, small oil economies, and eastern european countries, have the largest total carbon emissions per capita rates, when dividing the total emissions cumulated from 1859 to 2020 using the population size of 2020.

Government policy, or supranational policy, can affect economies and force sustainable practices and investments. France's large investments in nuclear energy make it a much cleaner economy in terms of carbon emissions, and other European countries have shifted to cleaner energy alternatives than oil after the OPEC oil crisis of 1970's.

In some countries, policies are not upheld or implemented fully, due to economic or political factors, in such cases the emissions rose as if unaffected by these policies. This was seen for India, which created the National Action Plan on Climate Change in 2008 but whose emissions have not subsided, as seen in Figure 8.

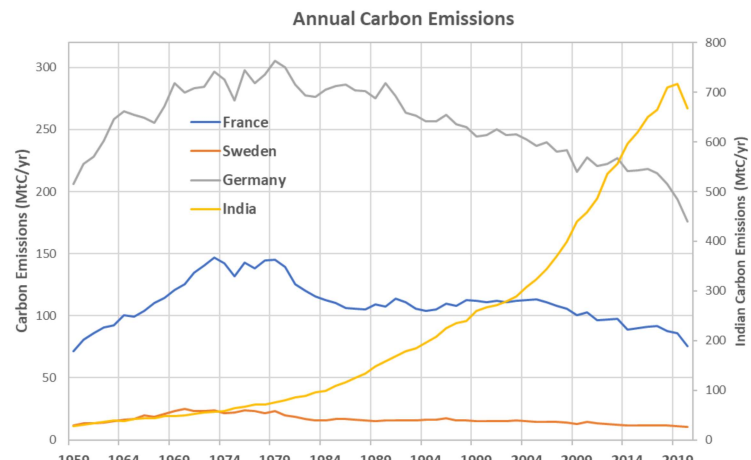


Figure 8: Yearly carbon emissions form 1959 to 2020 for France, Sweden, Germany, and India. Secondary axis is used for India due to the higher emission levels. Data from Friedlingstein et al.⁴.

Countries' emissions were impacted differently during 2020, as the COVID pandemic affected economies worldwide. Oman, Brunei, and China's emissions went up 2.3%, 2.0%, and 1.6% from 2019 to 2020. Around 30 small countries had an increase in carbon emissions in 2020 compared to 2019. Less populated countries included Samoa, Fiji, and the Maldives, while the more notable countries were Iran, Bahrain, Saudi Arabia, Pakistan, Afghanistan. The remaining countries had a decrease in emissions. Since a lot of countries are undergoing energy transitions, this is to be expected. For example, France went from 86 MtC in 219 to 76 MtC in 2020, but its emissions have been deducting steadily since the 1970s - with some stagnant exceptions. Germany had a 10 MtC/year decrease from 2019 to 2020, but this was also the case when comparing emission rates in 2014 and 2015.

Over the entire carbon emissions of 2019 of 10000 MtC globally, only a 5% decrease was noticed in 2020 levels, despite mass anthropological behavior change in transportation and consumption. The decrease cannot be entirely attributed to COVID, as the yearly rate of global emissions was on a downtrend.

CONCLUSION

In all, the increase in carbon emissions was shown through experimental atmospheric measurements and industrial models to be 1.5 to 2.8 ppm per year. If the increase in emissions continues, the doubling of carbon dioxide levels is estimated to cause an increase in surface temperature of 2.31°C. The observed sea level rise since 1880 can be attributed to only 3.7% of the Greenland ice sheet melting or alternatively, to an increase in temperature of the oceans by 0.70°C. Due to the increase in use of fossil fuels, and the grand amount of reserves left, it would take another 88 years to use the remaining fossil fuels, causing an increase of 2243.80GtCO₂ in the atmosphere. The countries with the most emissions per capita is the United States, and European emissions are on a downtrend, while countries like India are still increasing their emissions. The impact of climate change is therefore not negligible, and should be taken as seriously as possible, as it is necessary to divest from fossil fuels and adopt sustainable practices.

Bibliography:

1. S. Arrhenius. On the Influence of Carbonic Acid in the Air upon the Temperature of the Ground. *The London, Edinburgh, and Dublin Philosophical Magazine and Journal of Science*, pages 303–315, Apr. 1896. doi: 10.12987/9780300188479-028.
2. E. Foote. Circumstances Affecting the Heat of the Sun's Rays. *The American Journal of Science and Arts*, 22(66):383–384, 1856.
3. IPCC. Summary for policymakers. In V. Masson-Delmotte, P. Zhai, A. Pirani, S. L. Connors, C. P'ean, S. Berger, N. Caud, Y. Chen, L. Goldfarb, M. I. Gomis, M. Huang, K. Leitzell, E. Lonnoy, J. B. R. Matthews, T. K. Maycock, T. Waterfield, O. Yelekçi, R. Yu, and B. Zhou, editors, *Climate Change 2021: The Physical Science Basis. Contribution of Working Group I to the Sixth Assessment Report of the Intergovernmental Panel on Climate Change*. Cambridge University Press, Cambridge, UK and New York, NY, USA, 2021. doi: 10.1017/9781009157896.001.
4. Friedlingstein, P. et al. Global Carbon Budget 2024. *Earth Syst. Sci. Data Discuss.* 1–133 (2024) doi:10.5194/essd-2024-519.
5. F. Roquet, D. Ferreira, R. Caneill, D. Schlesinger, and G. Madec. Unique thermal expansion properties of water key to the formation of sea ice on Earth. *Science Advances*, 8(46): eabq0793, Nov. 2022. ISSN 2375-2548. doi: 10.1126/sciadv.abq0793.
6. Wetter und Klima - Deutscher Wetterdienst - Our services - Global maps of air pressure. Retrieved March 7, 2024, from https://dwd.de/EN/ourservices/global_air_pressure/luftdruckglobal.html
7. Team, G. W. Trends in CO₂ - NOAA Global Monitoring Laboratory. Retrieved January 17, 2024, from <https://gml.noaa.gov/ccgg/trends/index.html>.
8. Team, G. W. Dataset SPO co2 - NOAA Global Monitoring Laboratory. Retrieved January 17, 2024, from <https://gml.noaa.gov/data/dataset.php>
9. US EPA, O. Climate Change Indicators: Sea Level. Retrieved February 5, 2024, from [\(2016\)](https://www.epa.gov/climate-indicators/climate-change-indicators-sea-level).
10. NOAA (National Oceanic and Atmospheric Administration). (2024). Laboratory for Satellite Altimetry: Sea level rise. Retrieved March 1, 2024, from www.star.nesdis.noaa.gov/sod/lsa/SeaLevelRise/LSA_SLR_timeseries_global.php
11. CSIRO (Commonwealth Scientific and Industrial Research Organisation). (2017). Update to data originally published in: Church, J. A., & White, N. J. (2011). Sea-level rise from the late 19th to the early 21st century. *Surveys in Geophysics*, 32, 585–602. www.cmar.csiro.au/sealevel/sl_data_cmar.html
12. GISTEMP Team, 2025: GISS Surface Temperature Analysis (GISTEMP), version 4. NASA Goddard Institute for Space Studies. Dataset accessed by US EPA[9] at <https://data.giss.nasa.gov/gistemp/>.
13. numpy.polyfit — NumPy v2.2 Manual. <https://numpy.org/doc/stable/reference/generated/numpy.polyfit.html>
14. scipy.optimize.curve.fit — SciPy v1.15.2 Manual. https://docs.scipy.org/doc/scipy/reference/generated/scipy.optimize.curve_fit.html
15. US EPA, O. Greenhouse Gas Equivalencies Calculator - Calculations and References. Retrieved February 7th, 2024 from [\(2015\)](https://www.epa.gov/energy/greenhouse-gas-equivalencies-calculator-calculations-and-references)
16. OPEC Digital Publications - Annual Statistical Bulletin. Retrieved March 7, 2024 from <https://publications.opec.org/asb/chapter/show/123/2113>

Year	2016	2017	2018	2019	2020
Annual emissions (MtC/year)	9675	9804	10001	10016	9500
Variation rate from previous year	-	+1.3%	+2.0%	+0.01%	-5.0%

Table 1: Global emission rates from the World Bank, in MtC/year. Data from Friedlingstein et al.⁴ and the World Bank¹⁹.

17. 2024 Statistical Review of World Energy - British Petroleum. Retrieved February 7, 2024 from <https://www.bp.com/en/global/corporate/energy-economics.html>
18. Water Density | U.S. Geological Survey. Retrieved February 7, 2024 from <https://www.usgs.gov/special-topics/water-science-school/science/water-density>
19. Population, total | Data. Retrieved February 7, 2024 from <https://data.worldbank.org/indicator/SP.POP.TOTL>
20. Lee, C. & Wunch, D. Anthropogenic Climate Change, Advanced Physics Laboratory, Department of Physics, University of Toronto (2023).